S-transform time-frequency analysis of P300 reveals deficits in individuals diagnosed with alcoholism

Kevin A. Jones, Bernice Porjesz *, David Chorlian, Madhavi Rangaswamy,
Chella Kamarajan, Ajayan Padmanabhapillai, Arthur Stimus, Henri Begleiter

Neurodynamics Laboratory, Department of Psychiatry, SUNY Health Science Center, Brooklyn, New York, NY 11203, USA

Abstract

Objective: Decomposition of event-related potential (ERP) waveforms using time-frequency representations (TFR's) is becoming increasingly common in electrophysiology. The P300 potential is an important component of the ERP waveform and has been used to study cognition as well as psychiatric disorders such as alcoholism. In this work, we aim to further understand the nature of the event-related oscillation (ERO) components which form the P300 wave and how these components may be used to differentiate alcoholic individuals from controls.

Methods: The S-transform decomposition method is used to derive TFR's from single trial and trial-averaged ERP data acquired during a visual oddball task. These TFR's are averaged within time and frequency windows to provide ERO measures for further investigation. ERO measures are compared with conventional ERP amplitude measures using correlation analyses. Statistical analyses was performed with MANOVA and stepwise logistic regressions to contrast an age-matched sample of control ($N = 100$) and alcoholic male subjects ($N = 100$).

Results: The results indicate that the P300 waveform, elicited using infrequent salient stimuli, is composed of frontal θ and posterior δ activations. The frontal θ activation does not closely correspond to any of the conventional ERP components and is therefore best analyzed using spectral methods. Between group comparisons and group predictions indicate that the δ and θ band ERO's, which underlie the P300, show deficits in the alcoholic group. Additionally, each band contributes unique information to discriminate between the groups.

Conclusions: ERO measures which underlie and compose the P300 wave provide additional information to that offered by conventional ERP amplitude measures, and serve as useful genetic markers in the study of alcoholism.

Significance: Studying the ERP waveform using time-frequency analysis methods opens new avenues of research in electrophysiology which may lead to a better understanding of cognitive processes, lead to improved clinical diagnoses, and provide phenotypes/endophenotypes for genetic analyses.

© 2006 International Federation of Clinical Neurophysiology. Published by Elsevier Ireland Ltd. All rights reserved.

Keywords: EEG; Event-related potential; ERP; P300; Time-frequency representation; ERO; Alcoholism

1. Introduction

The P300 response is a well known and well studied phenomenon which represents an important correlate of higher cognitive brain processing. This response is defined as a positive electric potential deflection elicited approximately 300–500 ms following the occurrence of infrequent salient stimuli during an oddball paradigm. The P300 potential has been proposed to reflect attentional resource allocation, context updating (Donchin and Coles, 1988; Polich and Herbst, 2000) and context closure (Verlerger, 1988). The amplitude of the P300 has been associated with levels

---

* Corresponding author. Tel.: +1 718 270 2024; fax: +1 718 270 4081.
E-mail address: bp@cns.hscbklyn.edu (B. Porjesz).

of central nervous system inhibition, whereby inhibition of irrelevant networks accompanies excitation of the functionally relevant networks (Elbert and Rockstroh, 1987; Birbaumer et al., 1990; Fell et al., 1997). The P300 potential, therefore, represents an important measure of central nervous system processing of stimulus information.

In addition to providing a measure of cognitive behavior, the P300 amplitude is known to have clinical relevance (Polich and Herbst, 2000). For example, the visual P3b component, which corresponds to the P300 response with a maximal posterior distribution, shows reduced amplitude in individuals diagnosed with alcoholism (Porjesz and Begleiter, 1996; Porjesz et al., 1998). Similar effects have been observed in abstinent alcoholics (Porjesz and Begleiter, 1985) and in the offspring of alcoholics who can be considered at high risk to develop alcoholism (Begleiter et al., 1984; Porjesz and Begleiter, 1990; Berman et al., 1993; Hill and Steinhauer, 1993; Steinhauer and Hill, 1993; Ramachandran et al., 1996; van der Stelt, 1999). Therefore, in addition to the P300 amplitude having predictive capacity, it also has value as an index of vulnerability of alcoholism (Polich et al., 1994). These findings, along with evidence that the P300 amplitude is up to 60% heritable (O'Connor et al., 1994; Van Beijsterveldt and Boomsma, 1994; Van Beijsterveldt, 1996; Katsanis et al., 1997; Almasy et al., 1999), has led to utilization of the P300 amplitude as an endophenotype of the risk to develop alcoholism (and related disorders) and led to its use in genetic studies aimed at identifying risk alleles of alcoholism.

Increasing importance is now placed on the study of scalp-recorded neuroelectric oscillations in neurophysiology (Pfurtscheller and Lopes da Silva, 1999; Varela et al., 2001; Freeman, 2004a,b). This interest has stemmed from a recognition that different oscillatory responses may be attributed to different functional responses such as memory and integrative functions (Basar et al., 2001c). The form of these oscillations is expected to vary widely and research aimed at understanding how these forms might relate to the various cognitive functions is ongoing. For instance, there is increasing evidence to indicate that oscillations within specific frequency bands, ranging from δ (1–3 Hz) to γ (>28 Hz), are related to specific cognitive functions (Basar-Eroglu et al., 1996a; Basar et al., 1997, 1999, 2000, 2001c; Klimesch et al., 1997a, 2001; Schurmann et al., 1997; Schurmann and Basar, 1999; Doppelmayr et al., 2000; Sakowitz et al., 2000; Kolev et al., 2001; Rohm et al., 2001; Schurmann et al., 2001; Sauseng et al., 2002). We can expect that subtle cognitive responses will depend on the details regarding the timing of these oscillatory responses, their transitory nature, the spatial distribution of the oscillatory generators, phase synchronization, inter-frequency relations and other dynamic properties. Consequently, the application of new analytic methods in the study of these oscillations may reveal new insights into cognitive functioning. However, it is still an open question as to what extent evoked potentials are a result of stimulus generated modulations of ongoing oscillatory activity and

of stimulus generated impulses superimposed on ongoing activity. Our methodology, based on the analysis of oscillations, is an alternative method of describing the characteristics of the recorded signals; its results are not dependent on the exact neurophysiological causes of the measured scalp activity, and thus not dependent on the answer to the question about the nature of evoked potentials. The oscillations described here are those of a mathematical character implicit in any time-frequency analysis; to what extent they correspond to neurophysiological oscillations is not determinable from the data discussed here.

The application of time and frequency domain methods to the ERP has led to rich representations of the oscillatory components of these highly non-stationary waveforms and the analysis of both the time and frequency components of the ERP may contribute to a better neurophysiological understanding of stimulus-related brain functioning. Using such analysis methodologies, a number of authors have suggested that the P300 component is primarily formed by transient oscillatory events in the δ and θ frequency bands (Basar-Eroglu et al., 1992; Kolev et al., 1997; Yordanova et al., 2000, 2003; Schurmann et al., 2001). In a similar way the earlier arriving ERP components such as the N100, P200 and N200 have been shown to be primarily composed of high θ and α band oscillations (Klimesch, 1999; Klimesch et al., 2004; Gruber et al., 2005).

The exact mechanism of ERP formation through superposition of the component oscillations is still a matter of debate. The two main competing models of ERP formation within the oscillatory framework, are amplitude modulation, in which the ERP amplitude is modulated at a single trial level, or partial phase resetting, in which the phase of ongoing oscillations is reset following the stimulus presentation and amplitude enhancement occurs through trial averaging (Makeig et al., 2002; Penny et al., 2002). Recent data indicate that the phase resetting model is more important in the formation of early evoked components, such as the N100 (Makeig et al., 2002; Gruber et al., 2005); whereas, amplitude modulation has greater importance for the generation of the later ERP components, such as the P300 (Fell et al., 2004; Shah et al., 2004). However, these views are still subject to controversy (Yeung et al., 2004; Kirschfeld, 2005; Makinen et al., 2005). Regardless of the exact mechanisms underlying the formation of event related responses, the application of time-frequency analysis methods to EEG/ERP activity offers the ability to uniquely characterize these signals.

The major goal of this work is to represent P300 response in terms of the summation of oscillatory components, as elicited by salient stimuli during a visual oddball paradigm, to determine the characteristics of these components and show how they differ between alcoholic and control populations. This requires an understanding of the ERO measures themselves and how they relate to the conventional ERP amplitude measures. In Section 3.1 we examine the nature of the P300 wave and its frequency composition, consisting primarily of frontal θ band

oscillatory activity and posterior δ band activity. This leads to the analysis in Section 3.2 which is designed to investigate whether the ERO subcomponents of the P300 can differentiate the alcoholic group from the control group in a similar way to the P300 amplitude, i.e. with alcoholic individuals having less power than controls. Finally, logistic regression analyses, provided in Section 3.2, are designed to investigate if the multiple ERO subcomponents of the P300 offer unique and independent discriminatory information.

2. Methods

2.1. Subjects

The experimental subjects chosen for analysis were 100 alcoholic males with an age-range of 18–47 years (30.1 ± 5.3 years), and 100 age-matched normal male volunteers (29.6 ± 5.7 years) who served as controls. Alcoholics were diagnosed according to DSM IV criteria for alcohol dependence and were recruited from Kings County Hospital, New York. Prior to testing, they had been detoxified in a 30-day treatment program and none of the subjects was in the withdrawal phase. Controls were recruited either through notices posted in the SUNY Health Science Center, New York, or through newspaper advertisements. Only healthy volunteers without any personal and/or family history of major medical or psychiatric disorders and substance-related addictive illnesses were selected as control subjects. As an initial screening procedure, all the participants filled out a questionnaire containing details of personal and family history for medical, psychiatric and addictive disorders. However, alcoholic subjects with past history of psychiatric disorders and with comorbid diagnoses of substance use were also included in this study. The clinical data were obtained using the Bard/Porjesz adult alcoholism battery, a semi-structured clinical assessment schedule based on DSM IV criteria for the evaluation of clinical details of alcohol dependence and alcohol-related medical problems. Subjects were requested to abstain from alcohol and other central nervous system (CNS)-acting substances for 5 days prior to testing. A questionnaire, documenting drug use (alcohol, marijuana, cocaine, hallucinogens, methadone, tranquilizer, antidepressants, neuroleptics, other prescribed medications, nicotine and caffeine) over the previous 5 days prior to testing, was administered on the day of testing. Further, on the day of testing, all the subjects underwent a urine screen and breathalyzer test for the purpose of screening for recent drug use. Positive findings on these tests would exclude the subject's EEG data from any analyses. The Mini Mental State Examination (MMSE) (Folstein et al., 1975) was used to screen the participants for organicity. The subjects who had a history of major medical and neurological conditions including head injury, which would account for organicity, were also excluded from the study. All subjects had normal or corrected normal vision, and none reported hearing loss or impairment. An informed consent explaining the scope and methods of the study was also obtained before conducting the experiment. Experimental procedures and ethical guidelines were in accordance with approval from the Institutional Review Board (IRB).

2.2. Electrophysiological data acquisition

EEG activity was recorded using a 31-lead electrode cap (Electro-cap International, Inc.), Eaton, OH that included 19 channels of the 10–20 International System (Fp1, Fp2, F7, F3, Fz, F4, F8, T7, C3, Cz, C4, T8, P7, P3, Pz, P4, P8, O1 and O2) (Jasper, 1958) with 12 additional electrode locations (AF1, AF2, FC1, FC2, FC5, FC6, CP1, CP2, CP5, CP6, PO1 and PO2) following the American Electroencephalographic Society (1991). The electrodes were referenced to the nose and the ground electrode was placed on the forehead. The electrooculogram was recorded with horizontal and vertical leads placed at the outer canthus and supraorbitally on the left eye. The impedance was maintained below 5 kΩ. The signals were amplified with a gain of 10,000 by a set of amplifiers (Sensorium, Charlotte, VT) with bandpass of 0.02–100 Hz. The data were recorded on a Neuroscan system (Version 4.1) (Compumedics, Inc., El Paso, TX) with a sampling rate of 512 Hz. The subjects were seated in a comfortable, reclining chair located in a dimly-lit sound-attenuated RF-shielded room (IAC, Industrial Acoustics, Bronx, NY) and were instructed about the task and response requirements.

2.3. Experiment paradigm

The visual oddball paradigm employed by COGA has been previously described (Cohen et al., 1994). Three types of visual stimuli were presented: target (the letter X), non-target (squares), and novel (a different colored geometric figure on each trial). The probabilities of occurrence of the trials were 0.125 for the target trials, 0.75 for non-target trials and 0.125 for novel trials. Each stimulus shape subtended a visual angle of 2.5°. Stimulus duration was 60 ms, and the interstimulus interval was 1.6 s. Subjects were requested to respond to the target stimulus by pressing a button. Trials with baseline corrected amplitudes greater than 75 μV were marked as artifact contaminated and not analyzed further. The subject was presented with a total of 35 target stimuli, 210 non-target stimuli, and 35 novel stimuli trials. Subjects whose data did not contain a minimum of 20 artifact free trials in each condition were not selected for analysis. Fig. 1 summarizes the nature of the experiment paradigm and ERP data acquired. Fig. 1a is a representation of the experiment design depicting the three experiment conditions, the stimuli presentation and trial durations, subject response requirements and the trial presentation proportions. Fig. 1b depicts the layout of the 32 channel electrode montage on the scalp. Fig. 1c shows example grand-mean ERP waveforms elicited by the three stimuli conditions at the Pz electrode position (midline
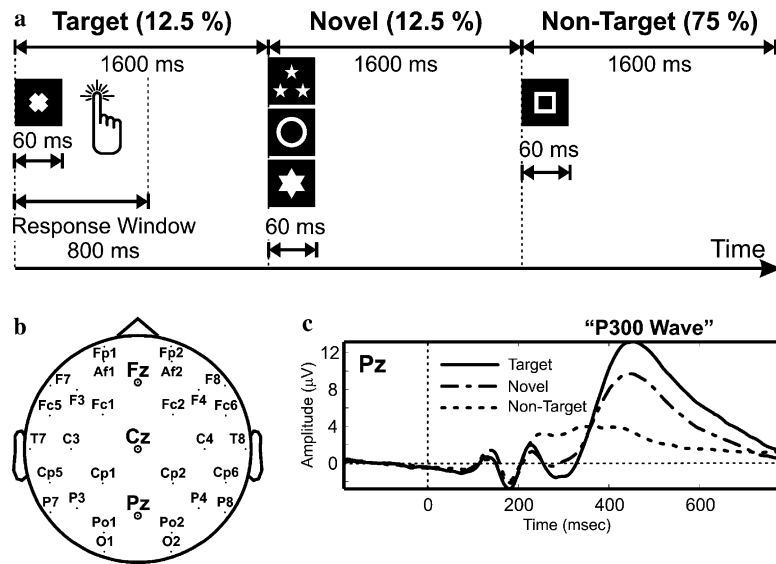
Fig. 1. Illustration of the visual event-related experiment design, setup and grand mean data. A pictorial representation of the experiment design is given in (a) which depicts the three trial conditions (target, non-target and novel), the trial presentation proportions, trial lengths and the response requirements. The 31 electrode scalp locations are shown in (b); the analysis presented here has focused on data from the Fz, Cz and Pz electrode sites. Grand mean event related waveforms are depicted in (c) for the Pz electrode (posterior midline) and the three experiment conditions. These grand mean waveforms were calculated using data from 100 control subjects. The target condition elicits the largest amplitude P300 event-related potential which is absent during the non-target condition.

posterior) and highlights the character of the event-related P300 wave which has its largest amplitude during the target condition. Target condition common stimulus single trial data from each subject were processed for analysis using the S-transform time-frequency representation (TFR). Additionally, ERP amplitude values were evaluated for each subject by 'peak-picking' the low-pass filtered (16 Hz) and baseline corrected trial-averaged event-related waveforms using a semi-automatic peak-picking program. The user of the program selected the appropriate time-windows for the peaks, and the program picked the extremum in the window; visual inspection allowed the user to adjust for ambiguities and ensure consistency between the peaks in different channels. Amplitudes were obtained for the N100, P200, N200 and P300 event-related components (cf. Fig. 4a). Waveforms that were ambiguous or artifact contaminated were omitted from the analysis. The components were analyzed in a within-group correlation analysis with ERO derived measures and between-group analysis of variance.

2.4. Time-frequency representation using the S-transform

Typical biological signals such as ERP responses are non-stationary in character, i.e., the statistical properties of the time-series vary as a function of time. This means that traditional methods of time-series analysis such as autoregressive methods and spectral analysis obtained via the Fourier transform are not readily applicable since they assume signal stationarity. In recent years attempts to address these problems have been made using methods of analysis based on time-frequency representations (TFR's)

of the signals. Some commonly applied TFR methods include the short-time Fourier transform (STFT); Cohen's class of generalized time-frequency distributions (GTFD) such as the Wigner-Ville distribution (WD); and the continuous wavelet transform (CWT). These methods provide a two-dimensional representation of the one-dimensional time-series which describes the signals local oscillatory behavior. These representations are redundant indicating that the points in the two-dimensional space are not independent. Each of these techniques offers differing strengths and weaknesses (Mitra and Pesaran, 1999).

In this work, we have applied a recently developed TFR technique termed the S-transform (Stockwell et al., 1996) to obtain estimates of localized power of the ERP time-series. The S-transform can be thought of as a generalization of the STFT (Gabor, 1946) and an extension to the CWT. The S-transform generates a time-frequency representation (TFR) of a signal by integrating the signal at each time point with a series of windowed harmonics of various frequencies as follows:

$$ST(t,f) = \int_{-\infty}^{\infty} h(\tau) \frac{|f|}{\sqrt{2\pi}} e^{-\frac{(t-\tau)^2 f^2}{2}} e^{-i2\pi f \tau} d\tau,$$

where $h(\tau)$ is the time-domain signal, f is frequency, t is a translation parameter, the first exponential is the window function, and the second exponential is the harmonic function. The S-transform TFR is computed by shifting the window function down the signal in time across a range of frequencies. The window function is Gaussian with $1/f^2$ variance and scales in width according to the examined frequency. This inverse dependence of the width of the Gaussian window with frequency provides the frequency-dependent

resolution (multiresolution). In effect the S-transform is a method of spectral localization with similarities to the continuous wavelet transform except using the concept of frequency instead of scale. The instantaneous amplitude (amplitude envelope) of the complex-valued S-transform TFR may be calculated by taking the absolute value $|ST(t, f)|$, the S-transform power is the square of the amplitude, while the absolutely referenced local phase information can be obtained using $\arctan(\Im[ST(t, f)] / \Re[ST(t, f)])$.

The S-transform derived measures used in the analysis presented here were obtained from the single trial and trial-averaged response. To obtain an estimate of event related total power response, ERO_{TOT} (stimulus onset phase locked plus non-phase locked oscillations), the squared instantaneous amplitudes (power) of the S-transform TFR were averaged across single trials for each individual. To obtain an estimate of event related phase-locked power response, ERO_{EVK}, the S-transform TFR power matrix was calculated for the averaged event-related response (single trial data averaged after alignment to the stimulus onset) per individual. Fig. 2 illustrates the calculation of the total and evoked response TFR power data for a single individual. The total power response, ERO_{TOT}, enhances events that occur in a similar time range as related to the stimulus onset and irrespective of their phase relations. The evoked response, ERO_{EVK}, enhances events which are phase-locked to the stimulus and reduces all other energy, including events which are subject to trial-to-trial temporal jitter. Fig. 3 depicts examples of grand-averaged TFR's of the visual oddball trial data calculated using Pz electrode data from 100 control subjects. The data are z-scored within each frequency and across

experiment trial type separately for each ERO measure type. It is evident from the TFR's shown in Fig. 3 that most energy is elicited in the first 700 ms after stimulus presentation. Also, the target and novel conditions evoke increased post-stimulus power in the lower frequency bands (<15 Hz) as compared to the non-target condition (the corresponding ERP waveforms are given in Fig. 1c). The ERO_{TOT} representation, when compared to the ERO_{EVK} data, show greater amounts of energy occurring throughout the trial period at both high and low frequencies. This reflects the inclusion of energy which is not phase locked to the stimulus onset in the ERO_{TOT} measure (total power response).

Average values were calculated for analysis from the S-transform power TFR within time-frequency regions of interest (TFROI's) (Lachaux et al., 2003) specified by five frequency band ranges and four time intervals given in Table 1. These frequency windows have been selected based on the well known 'natural frequencies' of brain rhythms (i.e., δ, θ, α, β and γ) which have been related in the literature to various cognitive functions and brain states (Basar et al., 2000). Specification of the time windows and further sub-windowing of the frequency bands was based on visual inspection of grand mean TFR data and the spatial distribution of grand mean ERO estimates over the scalp. The average time-frequency power values are then obtained using:

$$ERO_{TOT/EVK} = \langle TFR_{TFROI} \rangle$$

$$= \frac{1}{(t_{max} - t_{min})(f_{max} - f_{min})} \sum_{t_{min}}^{t_{max}} \sum_{f_{min}}^{f_{max}} |ST(t, f)|^2,$$
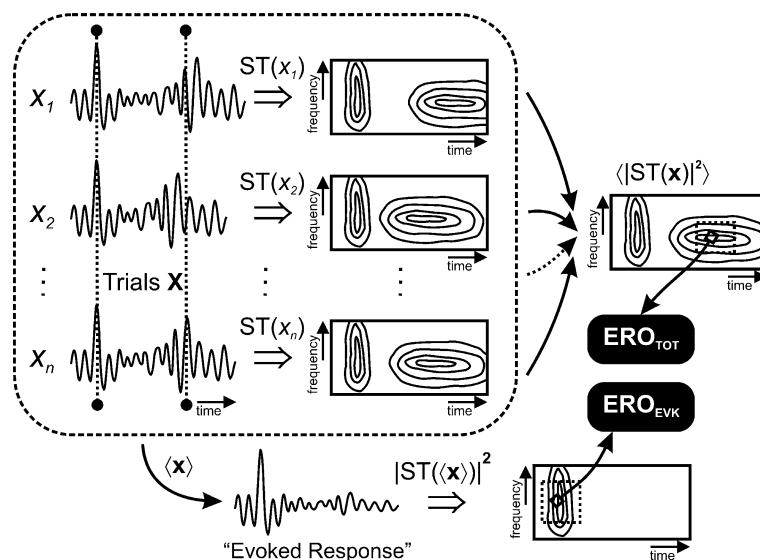
Fig. 2. Depiction of the event related oscillation (ERO) calculation methodology. Two types of ERO measure are obtained using the S-transform time-frequency representation (TFR): evoked power ERO (ERO_{EVK}) and total power (ERO_{TOT}). The ERO_{EVK} measure is calculated within a subject from the trial-averaged ERP response. Given enough trials this response will include only energy which is phase-locked to the stimulus onset since non-phase locked oscillations will be minimized by destructive interference. The ERO_{TOT} measure is calculated by averaging the S-transform TFR's of individual trials per subject. Since the ERO_{TOT} measure involves averaging of the amplitude envelope data (absolute value of the TFR) energy which is loosely time-locked to the stimulus onset will survive the averaging process. Time-frequency ERO values are obtained from the TFR's by averaging within windows specified in Table 1.
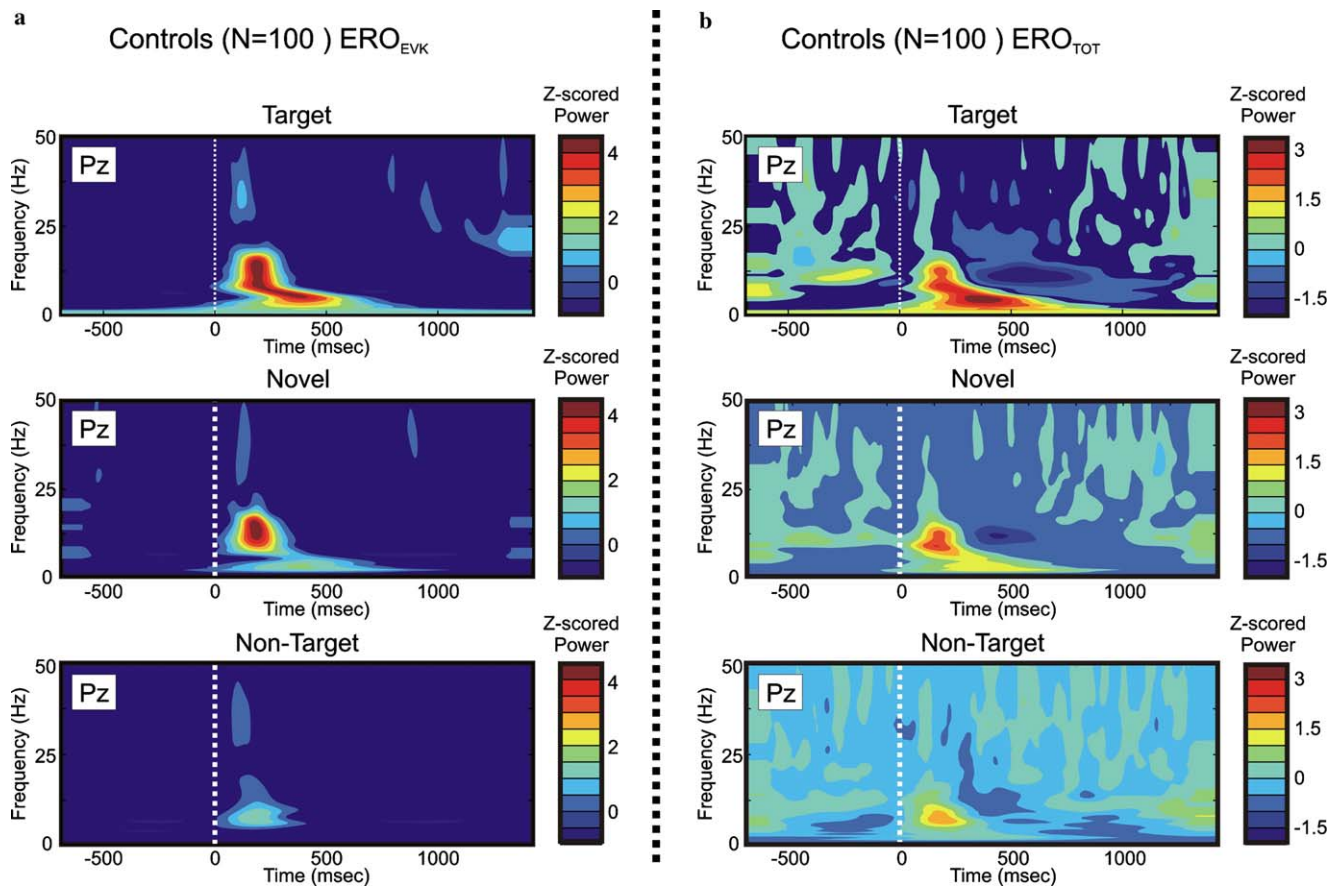
Fig. 3. Grand mean S-transform ERO time-frequency power representations of the three visual oddball experiment trial conditions (target, novel and non-target) using data from the Pz electrode of the control subjects (N = 100). The ERO_{EVK} measure is depicted in (a) while the alternative ERO_{TOT} measure is provided in (b). The data has been z-scored prior to plotting to allow comparison of high-frequency low-power energy with low-frequency higher-power energy. The z-scores were calculated within each ERO measure type and within each single frequency level but across each experiment condition. This form of scaling allows comparison of power, at each frequency-band, across condition and within each ERO measure.

where the ERO value is either the total response (ERO_{TOT}) or the evoked response (ERO_{EVK}) depending on the type of S-transform TFR matrix. This ERO calculation methodology is illustrated in Fig. 2 and is based on similar previously published methods (Tallon-Baudry and Bertrand, 1999). Code to calculate the S-transform TFR of one-dimensional signals has been made freely available by its author (Stockwell et al., 1996) and is available at http://www.co-ra.nwra.com/~stockwell.

2.5. Statistical analysis

A number of statistical techniques have been implemented to examine and explore the nature of ERO power values estimated from the target condition trial data (infrequent salient visual stimuli). These methods are briefly discussed in this section. The first part of the results section concentrates wholly on the control sample of data and is aimed at providing some understanding on the nature of

Table 1
ERO time-frequency regions of interest (TFROI) used for data analysis

ERO bands	Min. frequency (Hz)	Max. frequency (Hz)	Min. time (ms)	Min. time (ms)
δ_1 (1–2 Hz)	1	<2.5	300	700
δ_2 (3–3 Hz)	2.5	<3.5	300	700
θ_1 (4–5 Hz)	4	<5.5	200	500
θ_2 (6–7 Hz)	6	<7.5	200	400
α (8–12 Hz)	8	< 11.5	100	300

Mean power values were extracted using the S-transform time-frequency representation (TFR) within time and frequency ranges outlined in the table. These TFROI were defined using visual inspection of grand-mean data as discussed in the methods section.

low-frequency ERO measures which are evoked following stimulus presentation. In particular we apply correlation analysis to examine the extent of similarities between the derived ERO measures with traditional ERP amplitude 'peak-pick' values corresponding to the N100, P200, N200 and P300 event related potentials. The Pearson correlation coefficient was used to test the significance of the observed correlation coefficients. Since these tests, and subsequent between-group parametric tests assume the data is Gaussian, tests of normality were performed on the ERO and ERP amplitude data using the one-sample Kolmogorov–Smirnov test. It was found that the N100, P200 and N200 ERP amplitudes were normally distributed without need for transformation, however, the P300 ERP amplitude and ERO measures required log transformation to achieve normality.

Since the P300 'wave' is relevant in the study of alcoholism and related disorders we use the S-transform time-frequency method to obtain time-local power spectra, at the mean P300 peak latency, to estimate the approximate relative contributions of the low frequency components to the P300 wave. The multi-resolution property of the S-transform allows the time-local power spectra to simultaneously capture high frequency short-time (local) energy as well as low frequency long-time (broad) energy; therefore, use of the S-transform time-local power spectrum allows an estimate of the relative contributions of transient evoked low frequency oscillations which compose the P300 wave. This feature of the S-transform, along with the ability to invert the S-transform time-local Fourier spectrum coefficients into one-dimensional time-local time series, leads to the notion of time-time analysis using the TT-transform (Pinnegar and Mansinha, 2003).

The second and main part of the results section deals with between-group comparisons of the S-transform derived ERO data and ERP amplitudes using target condition trials of the visual oddball paradigm. Initial tests of group differences were applied to three midline electrodes (Fz, Cz and Pz) using multivariate analysis of variance (MANOVA). These three electrodes were chosen for statistical analysis since examination of the spatial distributions of θ and δ band ERO data indicate maximal power is observed both in the fronto-central or parieto-central locations and along the midline. MANOVA tests are applied since in the first stage of the analyses we are interested in determining which frequency band and/or ERP components may act as useful predictors of the alcoholic status. Also, MANOVA is an appropriate test since measures derived from the scalp electrodes are expected to be highly correlated in part due to the effects of volume conduction in cerebrospinal fluid, skull and scalp (Nunez, 1981). Group differences were assessed using the Pillai-Bartlett trace to evaluate an *F*-value and corresponding significance level. MANOVA tests were applied to evoked power ERO (ERO$_{EVK}$) and total power ERO (ERO$_{TOT}$) data for each frequency band (see Table 1) separately ($\delta1$, $\delta2$, $\theta1$, $\theta2$ and α) and for each ERP component separately (N100, P200, N200 and P300). Since the control and alcoholic subjects

were age and gender matched these data were not added as covariates in the statistical model.

Frequency bands and ERP amplitudes, identified using MANOVA, which predict subject group status are further analyzed using stepwise logistic regression analysis in which we model the group variable using multiple frequency ERO data and ERP data from the three midline electrode locations simultaneously. The logistic regression models were iteratively adjusted by adding and dropping terms to determine the 'best' and most parsimonious model using Akaike's Information Criterion (AIC). The AIC measure penalizes the residual sum of squares by two times the number of parameters in the model multiplied by the residual mean square of the initial model. All *p*-values are provided without correction for multiple testing since the work presented here is intended to be exploratory in nature.

3. Results

The focus of the data analysis is twofold. Firstly, we are interested in providing additional understanding of the nature of ERO components which underlie and comprise the ERP components, and in particular the P300 wave since this amplitude of the P300 components is known to be reduced in alcoholics (Section 3.1). The second part of the analysis section (Section 3.2) deals with assessing the usefulness of the ERO measures analyzed in Section 3.2 as predictors of group classification of the control and alcoholic subjects. The group-wise analysis presented in Section 3.2 leads to the development and assessment of a 'best predictor' of alcoholism diagnosis using a combination of ERO measures which compose the P300 wave.

3.1. ERO time-space-frequency characteristics in the control group

In this section, we examine the time, frequency and spatial properties of ERO's extracted from target condition trials using the control data sample. The results of this analysis provide greater understanding of the nature of these oscillations.

3.1.1. Examination of the dynamics of ERO power

Fig. 4 shows an example of grand-mean ERP and ERO$_{EVK}$ data derived from the control sample of subjects (grand average of data collected from 100 individuals). Fig. 4a displays the grand mean target-condition ERP waveform acquired at the Cz electrode position. Included in Fig. 4a are the contoured spatial distributions (head plots) of ERP amplitude measures formed by plotting the averaged amplitudes (averaged across control subjects) at the respective electrode positions (cf. Fig. 1b). Fig. 4b is the log-transformed TFR of the ERP waveform depicted in Fig. 4a in which the TFR distributions corresponding to the mean-response ERP were averaged across individuals. Also shown in Fig. 4b are the contoured spatial distri-
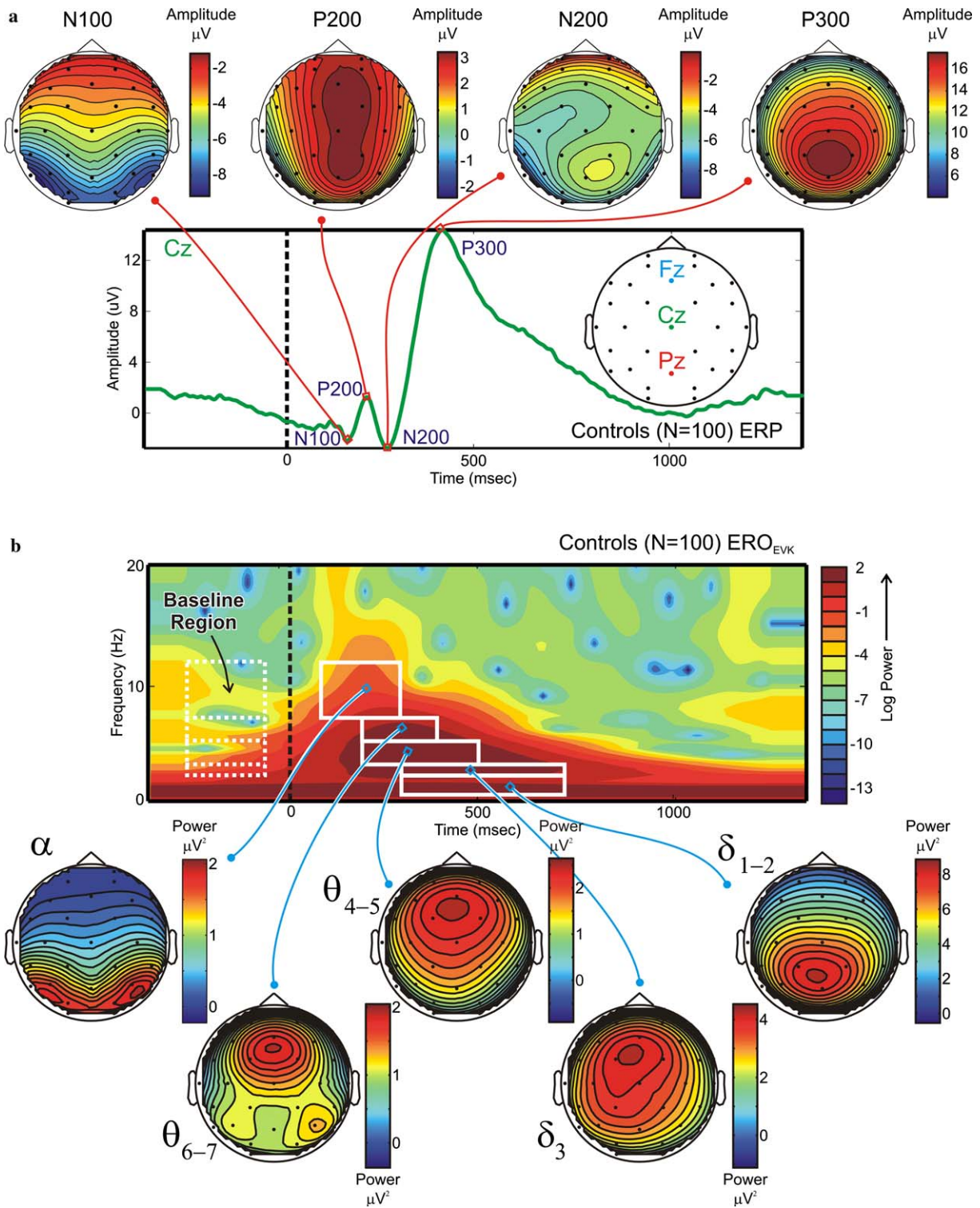
Fig. 4. Comparison of ERP and ERO measures derived from the target condition data of 100 control subjects. The grand mean ERP waveform for the Cz electrode (central midline) is depicted in (a) along with the grand mean spatial distributions of the target condition ERP components: N100, P200, N200 and P300. The grand-mean S-transform evoked TFR for the Cz electrode is shown in (b) with the grand mean ERO_{EVK} spatial distributions for the TFROI windows given in Table 1. The spatial distribution of the α band ERO has a similar shape to the N100 spatial distribution (the opposing color gradient is due to the negative ERP amplitude values). Also, the spatial distribution of the lower δ band ERO has a similar shape to the P300 spatial distribution. However, the frontally distributed upper δ and theta band ERO data do not have a clear coincidence with the ERP amplitude spatial distributions. (Blue values in the plots are smaller in magnitude than red values.)

butions of the average time-frequency power values (ERO_{EVK}) calculated at the TFROI's defined in Table 1 and plotted at the respective electrode positions. The time windows used for each of the frequency bands are modified to encompass the transient peak post-stimulus power within that frequency band. Hence, the time windows become tighter and earlier as the frequency bands increase to reflect the fact that in general the higher frequency oscillations have peak power earlier in the ERP than lower frequencies. At the lowest frequency (δ_{1-2}), however, there is very poor time resolution (one to half a second resolution); this is an artifact of the Fourier based analysis method and the time window of 300–700 ms was selected to encompass the approximate temporal location of the P300 wave. It is recognized, however, that these window selections may be suboptimal and may be adjusted for each electrode position, for each experiment condition, for different experiment paradigms, and per individual. Nevertheless, these window selections allow a preliminary analysis of the general dynamics of ERO's during the target condition of the visual oddball experiment.

3.1.2. Comparative analysis of ERP amplitudes and ERO power

A visual comparison of the spatial distributions of ERP component amplitudes (Fig. 4a) and ERO's (Fig. 4b) reveals close similarity between the spatial distributions of α ERO powers with the N100 amplitude and lower δ ERO powers (δ_{1-2}) with the P300 amplitude. The frontally distributed theta (θ_{4-5} and θ_{6-7}) and upper δ (δ_{3-3}) ERO's do not show a simple correspondence with either of the ERP amplitude spatial distributions. This suggests that this frontally distributed ERO activity, which primarily constitutes the early part of the P300 wave as well as the N200 component, cannot be directly quantified using the ERP amplitude measures. This conclusion is supported by the correlation analysis (Table 2) of ERO_{EVK} power data with ERP amplitudes estimated from the Fz, Cz and Pz electrodes (frontal, central and parietal midline) within the control sample of subjects. The correlation results summarized in Table 2 indicate that there is high correlation between ERO_{EVK} lower δ power and P300 amplitude with strongest correlation for the Pz electrode ($\rho = 0.81$). There is also indication of moderate to high correlation of ERO_{EVK} lower α power at the Pz electrode with the N100 ERP amplitude ($\rho = 0.55$). The highest correlation for the lower theta ERO_{EVK} power is found to be with the N200 ERP amplitude at the Cz electrode position ($\rho = 0.45$), however, as shown in Fig. 4a the spatial distribution of these measures is not similar and therefore they cannot be regarded as being equivalent. The maximum correlation observed for the upper θ ERO_{EVK} power is with the P200 ERP amplitude at the Fz electrode; although the spatial distribution of this ERP component is approximately fronto-centrally distributed the correlation coefficient is moderate to weak ($\rho = 0.36$). An important conclusion drawn from these correlation analyses is that the frontally distributed θ band ERO measure cannot be simply quantified using traditional ERP amplitude measures.

3.1.3. Decomposition of the P300 waveform

The correlation analysis given in Table 2 reveals moderate correlation between P300 ERP amplitude and ERO_{EVK} θ powers (ρ between 0.4 and 0.6) indicating that the P300

Table 2
Pearson's product moment correlation coefficients (ρ) describing the relationship between target condition visual oddball event-related potential (ERP) amplitudes and evoked event-related oscillation (ERO_{EVK}) measures at three electrode positions (Fz, Cz and Pz) using the control subset of data ($N = 100$)

	P3	N2	P2	N1
Fz electrode				
δ_1 (1–2 Hz, 300–700 ms)	**.742**[***]	.136	.198[*]	−.197[*]
δ_2 (3–3 Hz, 300–700 ms)	.636[***]	−.354[***]	−.026	−.211[*]
θ_1 (4–5 Hz, 200–500 ms)	.606[***]	−**.421**[***]	.113	−.223[*]
θ_2 (6–7 Hz, 200–400 ms)	.558[***]	−.236[*]	**.363**[***]	−.311[**]
α (8–12 Hz, 100–300 ms)	.523[***]	−.163	.271[**]	−**.398**[***]
Cz electrode				
δ_1 (1–2 Hz, 300–700 ms)	**.772**[***]	.028	.112	−.219[*]
δ_2 (3–3 Hz, 300–700 ms)	.533[***]	−.397[***]	−.205[*]	−.332[***]
θ_1 (4–5 Hz, 200–500 ms)	.486[***]	−**.451**[***]	−.124	−.334[***]
θ_2 (6–7 Hz, 200–400 ms)	.531[***]	−.101	**.296**[**]	−.376[***]
α (8–12 Hz, 100–300 ms)	.446[***]	−.081	.268[**]	−**.501**[***]
Pz electrode				
δ_1 (1–2 Hz, 300–700 ms)	**.81**[***]	.035	.052	−.09
δ_2 (3–3 Hz, 300–700 ms)	.592[***]	−**.336**[***]	−.162	−.207[*]
θ_1 (4–5 Hz, 200–500 ms)	.553[***]	.291[**]	−.056	−.153
θ_2 (6–7 Hz, 200–400 ms)	.420[***]	−0.006	**.336**[***]	−.339[***]
α (8–12 Hz, 100–300 ms)	.268[**]	−.206[*]	.221[*]	−**.55**[***]

Post-stimulus mean ERO_{EVK} power estimates were calculated using the frequency specific time windows outlined in Table 1. ERO power data and P300 ERP amplitudes were log transformed to achieve normality. Coefficients denoted with [*] are significant at the 0.05 level using a two-tailed test; coefficients denoted with [**] are significant at the 0.01 level; coefficients denoted with [***] are significant at the 0.001 level. *P*-values are presented without correction for multiple testing. Coefficients highlighted in bold denote the largest correlation coefficient for the ERP amplitudes at each electrode location.

wave amplitude is to an extent dependent upon the magnitude of the earlier arriving theta band oscillations. This fits the view that P300 responses are primarily the outcome of oscillatory changes in δ and θ oscillations during stimulus processing and therefore these rhythms form the P300 wave (Stampfer and Basar, 1985; Basar-Eroglu and Basar, 1991; Yordanova and Kolev, 1996; Demiralp et al., 1999). As discussed in the methods section the S-transform provides time-local power spectra which may be used to quantify the proportions of the oscillatory components which influence the time-series at that time point. Fig. 5 shows the time-local spectral decomposition of the P300 wave estimated using the S-transform data at the grand-mean P300 peak latency (430 ms). Fig. 5e displays the relative proportions of frequencies in the 1 to 7 Hz range (δ and θ bands) for the Fz, Cz and Pz electrodes (normalized to add to 100 % within this frequency range). The relative proportions of δ and θ band oscillations composing the P300 wave are also shown in Fig. 5e. These values indicate that the proportions vary according to electrode position in

a similar pattern as suggested in previous reports (Karakas et al., 2000); with approximately equal proportions at the frontal electrode site and higher δ proportions at the posterior location. It is also evident from Fig. 5e that the fronto-parietal power distribution varies with frequency. Oscillations below 3 Hz have maximum power distribution in the posterior electrodes, whereas oscillations 3 Hz and greater show maximal power in the frontal electrodes; this effect is also evident from the ERO head plots of Fig. 4b and supports the notion of a multiple loci of oscillatory activity comprising the P300 wave (and the earlier N200 component), i.e., frontal θ and posterior δ.

3.2. Between group analyses

3.2.1. MANOVA analysis of ERP amplitude and ERO power

Results of the MANOVA analyses are provided in Table 3; in these analyses the log transformed ERO power and ERP amplitude dependent variables (from the Fz, Cz
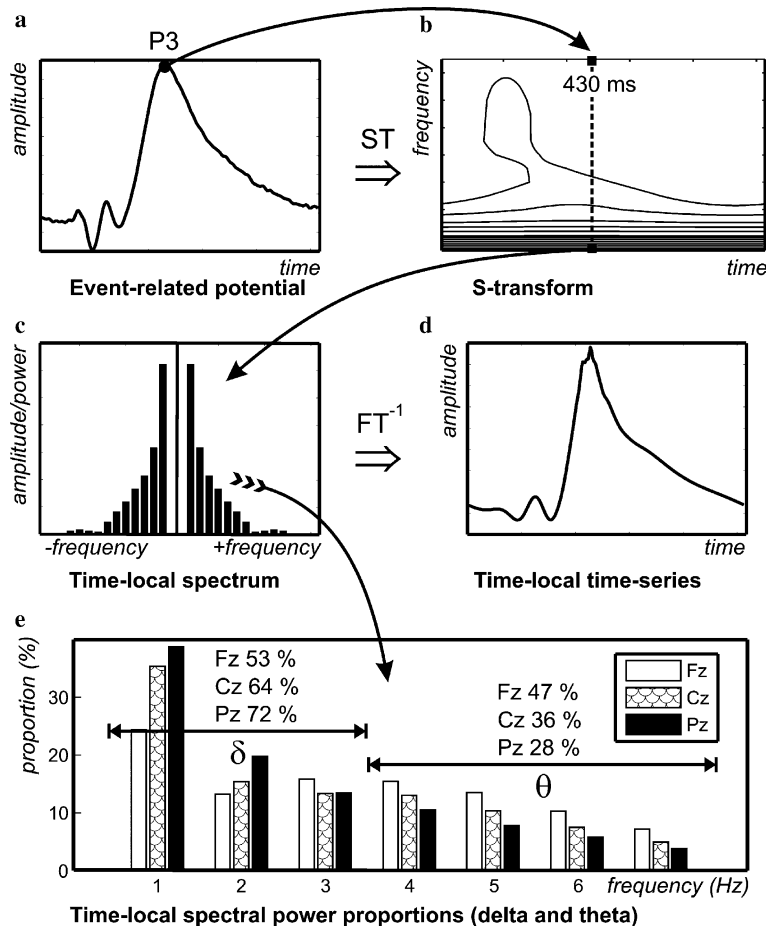
Fig. 5. Decomposition of the grand mean P300 wave into its constituent low frequency oscillations using the S-transform derived time-local power spectrum. An example grand mean ERO waveform is depicted in (a) for the Pz electrode and calculated from the control subject dataset (100 subjects). A pictorial representation of the ERP waveform S-transform TFR is shown in (b). The time-local power spectrum extracted from the S-transform TFR at the average P300 peak latency is plotted in (c). The inverse transform of the time-local Fourier spectrum results in the time-local time-series depicted in (d). The time-local power spectrum is used to derive single frequency spectral powers which are relevant to the shape of the P300 wave at that time. The relative proportions of these local spectral powers are plotted in (e).

Table 3

Results of MANOVA statistical tests of group significance using log transformed ERO_{EVK}, ERO_{TOT} and ERP amplitude data (log transformed P300 amplitude)

	Model: log(Fz), log(Cz), log(Pz) $\sim$ Group ($N = 200$, $df = 196$)		
	df	*Pillai-Bartlett trace*	*F-value*
ERO_{EVK}			
δ_1 (1–2 Hz, 300–700 ms)	**1**	**0.167**	**13.0******
δ_2 (3–3 Hz, 300–700 ms)	1	0.102 (0.074)	7.5*** (5.2**)
θ_1 (4–5 Hz, 200–500 ms)	1	0.113 (0.099)	8.3*** (7.2***)
θ_2 (6–7 Hz, 200–400 ms)	1	0.069 (0.097)	4.8** (7.0***)
α (8–12 Hz, 100–300 ms)	1	0.027 (0.037)	1.8 (2.5)
ERO_{TOT}			
δ_1 (1–2 Hz, 300–700 ms)	1	0.103	7.5***
δ_2 (3–3 Hz, 300–700 ms)	1	0.076 (0.07)	5.4** (4.9**)
θ_1 (4–5 Hz, 200–500 ms)	**1**	**0.146 (0.13)**	**11.1****** (9.8***)
θ_2 (6–7 Hz, 200–400 ms)	1	0.063 (0.1)	4.4** (7.34***)
α (8–12 Hz, 100–300 ms)	1	0.002 (0.03)	1.0 (1.9)
ERP amplitude			
P300	1	0.127	9.6***
	Model: Fz, Cz, Pz $\sim$ Group ($N = 200$, $df = 196$)		
ERP amplitude			
N100	1	0.023	1.6
P200	1	0.047	3.2*
N200	1	0.027	1.8

Pillai-Bartlett trace and *F*-values in brackets indicate ERO model results using baseline corrected data in which mean values extracted from the pre-stimulus region of the TFR data are subtracted from the post-stimulus ERO power estimate data. Baseline correction is not applied to the δ_1 (1–2 Hz) ERO data due to the poor temporal resolution afforded by the Stockwell transform at these low frequencies. The Pillai-Bartlett trace is the sum of explained variances on the discriminant variates and is used to calculate the approximate *F*-value. *F*-values denoted with * are significant at the 0.05 *p*-value level using a two-tailed test; *F*-values denoted with ** are significant at the 0.01 *p*-value level; *F*-values denoted with *** are significant at the 0.001 *p*-value level (N=200). *P*-values are uncorrected for multiple tests. *F*-values highlighted in bold denote the largest *F*-values within each ERO measure.

and Pz electrodes) were modeled with group (alcoholic or control) as the independent variable. Modeling was applied to each frequency band ERP measure separately to assess which frequency bands and components act as discriminators of the group. Alcoholic individuals revealed significantly less ERO_{EVK} and ERO_{TOT} power in the delta (δ_{1-2} and δ_{3-3}) and theta (θ_{4-5} and θ_{6-7}) bands but not in the α band. In concordance with previously published work alcoholic individuals were observed to manifest lower P300 amplitude. The N100 and N200 amplitudes were not significantly different between the

groups, whilst the P200 component was marginally significantly different (with lower amplitudes in the alcoholic group); however, significance is not retained after Bonferroni correction for multiple testing. The maximum *F*-values for each of ERO powers suggests that the δ band is the better discriminator using the ERO_{EVK} measure, whereas the θ band is the superior group discriminator using the ERO_{TOT} measure. A similar pattern of results is observed using ERO data which have been baseline modified using the baseline ERO time-windows pictured in Fig. 4b and detailed by results in brackets in Table 3.

Table 4

Results of a stepwise logistic regression analysis of δ_1 and θ_1 band ERO data and the P300 ERP amplitude using the three midline electrodes (Fz, Cz and Pz) as predictor variables

	Model: Group $\sim$ log(Fz) + log(Cz) + log(Pz) ($N = 200$, null $df = 198$, null deviance = 277.3)			
	df	*Retained terms*	*Term deviance*	*p-value (χ^2)*
ERO_{EVK}				
δ_1 (1–2 Hz, 300–700 ms)	1	log(Fz)	35.0	3.3×10^{-9}***
θ_1 (4–5 Hz, 200–500 ms)	1	log(Fz)	23.8	1.1×10^{-6}***
ERO_{TOT}				
δ_1 (1–2 Hz, 300–700 ms)	1	log (Cz)	21.0	4.6×10^{-6}***
θ_1 (4–5 Hz, 200–500 ms)	1	log(Fz)	28.8	8.2×10^{-8}***
ERP amplitude				
P300	1	log(Fz)	22.8	1.8×10^{-6}***

The stepwise selection of variables is achieved using AIC. For each logistic model examined the most parsimonious model included data from a single electrode. *P*-values denoted with *** are significant at the 0.001 *p*-value level ($N = 200$). *P*-values are uncorrected for multiple tests.

Table 5
Results of a stepwise logistic regression analysis of combined ERP P300 amplitude data and δ_1 and θ_1 band ERO_{EVK} and ERO_{TOT} data

Combined P300 ERO Model	Model: Group ~ log(Fz-P300) + log(Fz-δ_1) + log(Fz-θ_1) ($N = 200$, null $df = 198$, null deviance = 277.3)			
	df	Retained terms	Term deviance	p-value (χ^2)
Fz-P300 amplitude and	1	log(Fz-δ_1)	35.0	3.3×10^{-9}***
Fz-δ_1 (ERO_{EVK}) and	1	log(Fz-θ_1)	14.4	0.00014***
Fz-θ_1 (ERO_{TOT})				

The stepwise selection of variables is achieved using AIC. Two variables are retained after analysis using the logistic regression analysis summarized in Table 5: δ_1 band ERO_{EVK} data from the Fz electrode (Fz-δ_1) and θ_1 band ERO_{TOT} data from the Fz electrode (Fz-θ_1). P-values denoted with *** are significant at the 0.001 p-value level ($N = 200$). P-values are uncorrected for multiple tests.

Due to the poor temporal resolution of the lowest frequencies the baseline modified version of the δ_{1-2} band is not provided. Also, we note that similar MANOVA analysis of the baseline region low frequency ERO data (excluding δ band data) did not reveal significant between-group differences.

3.2.2. Stepwise logistic regression analysis of ERP amplitude and ERO power

The results of separate stepwise logistic regression analysis for ERO_{EVK} (δ_{1-2} and θ_{4-5}), ERO_{TOT} (δ_{1-2} and θ_{4-5}), and P300 amplitude data are summarized in Table 4. Each test incorporates data from a single band or component amplitude and the three midline electrodes (Fz, Cz and Pz). Retained terms, corresponding to electrode positions, for the most parsimonious model in each test are provided in Table 3. In each case, the most parsimonious model uses data from a single electrode suggesting that adding data from the neighboring electrodes does not improve the discriminatory power of the model. The Fz electrode is retained for all measures except for ERO_{TOT} δ_{1-2} power which selects data from the Cz electrode. The results of these stepwise logistic regression tests concur with the MANOVA based tests which suggest that the δ band data provides greater group discrimination using ERO_{EVK} while the θ band offers better discrimination using ERO_{TOT} data. In the next section results of a stepwise logistic regression model are presented using combined ERO and ERP data as input.

3.2.3. Logistic regression analysis of combined ERO_{EVK} δ and ERO_{TOT} θ powers

Results from the previous MANOVA and logistic regression analysis suggest that a combination of δ ERO_{EVK} and theta ERO_{TOT} band measures may offer increased discriminatory power than the traditional ERP P300 amplitude measure. To test this possibility a combined stepwise logistic regression model was performed which included P300 amplitude, ERO_{EVK} δ and ERO_{TOT} θ derived from the Fz electrode. The retained terms for this model are given in Table 5. The P300 ERP amplitude is not retained within the most parsimonious model; however, both θ and δ band ERO measures are retained indicating that these ERO measures encompass the P300 amplitude group effect and that the δ and theta band measures offer

unique and independent information in the model. The δ ERO_{EVK} measure explains a greater proportion of the model deviance than the θ ERO_{TOT} measure; however, a significant portion of the deviance is explained solely by the θ measure. Fig. 6 depicts the modeled ERO data in the control and alcoholic groups at the Fz electrode and the spatial distributions of these measures.

4. Discussion

The present study was designed to examine the usefulness of measures derived from the S-transform method of time-frequency analysis in revealing the components (ERO's) which compose the ERP waveform, and the efficacy of these measures in discriminating the alcoholic and control population. It must be emphasized that these components do not necessarily represent distinct neurophysiological processes but are a representation of the recorded scalp signals. The results of these analyses indicate that a frontally focused θ band activity (4–5 Hz) and a posterior distributed δ band activity constitute the P300 ERP waveform, with the θ component forming the N200 and the early part of the P300 wave, and the δ component forming the main part of the P300 wave. Component ERO's have been derived from two different signal types, the single-trial signals, and the averaged signals, resulting in the total power ERO_{TOT} and the evoked ERO_{EVK}. The statistical analysis suggests that the ERO_{TOT} measure of the θ component is the better group discriminator than the equivalent ERO_{EVK} measure. The opposite situation is indicated for the δ band component with the ERO_{EVK} measure acting as the better group discriminator. A similar finding is reported in a study from our laboratory of adolescent offspring of alcoholic individuals using the same experiment paradigm and TFR methodology (Rangaswamy et al., 2005). In this offspring study, it was reported that high risk adolescents show power deficiencies in both δ and θ bands; however, δ band differences were stronger using the ERO_{EVK} measure while θ differences were only observed using the ERO_{TOT} measure. One possible interpretation of the θ band findings is related to slight trial-to-trial temporal jitter (variation). Trial-averaging of the ERP waveform will diminish imperfectly phase-locked θ band oscillations in the ERO_{EVK} measure while the ERO_{TOT} measure will retain this energy and therefore provide a
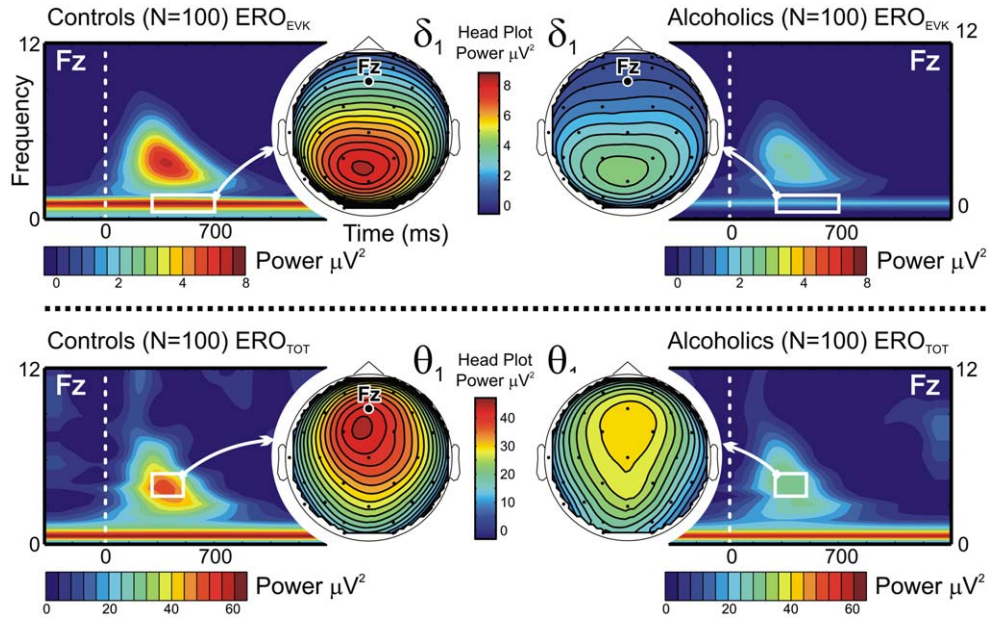
Fig. 6. Representation of the ERO data used to discriminate the control and alcoholic populations. Lower δ band (δ_{1-2}) ERO_{EVK} data and lower θ band (θ_{4-5}) ERO_{TOT} data are found to be useful predictors of group membership. Alcoholic subjects are shown to manifest deficient power for these ERO measures in a similar way to the amplitude deficiencies observed for the P300 ERP component. Illustrations of these power deficits, and the spatial distributions of the ERO measures, are illustrated.

better estimate of evoked θ ERO's. Trial-to-trial temporal jitter is less likely to affect the averaging of the lower frequency δ band oscillations, due to the lower temporal resolution, therefore the ERO_{EVK} measure may adequately represent the δ ERO's. In this case we expect the ERO_{TOT} and ERO_{EVK} forms of the δ ERO's to give similar group differences; however, the ERO_{EVK} measure shows stronger group differences. We speculate that in contrast to the θ ERO measure, where trial-averaging negatively impacts the measure due of trial-to-trial temporal variation, trial averaging improves quantification of the delta ERO possibly through suppression of noise in the δ frequency band and/or irrelevant non-phase locked activity.

The θ band ERO_{TOT} group differences reported here reveal stronger group effects with the frontal (Fz) electrode when compared to the central (Cz) and posterior (Pz) electrodes. These findings coincide with the observation that the θ ERO is a frontally distributed (c.f Figs. 4b and 6) and indicate that the maximal group differences occurs at the location of maximum θ ERO. The delta ERO_{EVK} measure, which has a centro-parietal distribution, reveals strongest group differences also with the frontal electrode (Fz), although the effect is also significant at the Cz and Pz electrode locations. These widespread power differences are in agreement with the concept that lower frequency oscillations are more widespread and hence involved in wider range communication between neural assemblies (von Stein and Sarnthein, 2000). Also, we note that the reference-dependent nature of the data being examined makes interpretation of the location of 'strongest effects' imprecise. Another study which has reported θ and δ ERO deficits in adult alcoholics used ERP waveforms elicited with a

Go-Nogo task (Kamarajan et al., 2004). This study employed a matching pursuit algorithm to obtain the TFR's of the single trial data which were used to calculate the θ and δ band ERO_{TOT} measures. For the Go condition strong δ band ERO differences were observed over frontal, parietal and occipital locations, however, θ band differences were not observed for the Go condition. The Nogo condition revealed strong δ and θ band ERO differences. The δ band differences were again widespread, whereas the θ band differences were focused in frontal electrode positions. The widespread nature of the δ band ERO effects and the more frontally localized θ band differences are in good agreement with the results reported here. However, the strongest differences in the Go-Nogo experiment data were observed for the Nogo condition which the authors suggest represents a deficient inhibitory control and information-processing mechanism in the alcoholic subjects (Kamarajan et al., 2004).

Results from the previously discussed studies support the suggestion that ERO's can be discerned in a number of cognitive functions, with time-courses that vary according to the required task. In the literature, neural oscillatory responses have been attributed to various cognitive processes. For instance, δ responses are considered to mediate signal detection and decision-making (Basar et al., 1999; Schurmann et al., 2001), while θ rhythms have been attributed with attention, recognition memory, and episodic retrieval (Doppelmayr et al., 1998; Gevins et al., 1998; Basar et al., 2001a; Klimesch et al., 2001). Slow α wave oscillations have been associated with the attribution of attentional resources and fast α with semantic memory and stimulus processing (Klimesch et al., 1994, 1997a,b,

1998; Basar et al., 1997). Beta and gamma frequency oscillations are regarded as important building blocks of brain activity and have been attributed to a diverse range of processes, including cognitive integrative functions (such as 'binding'), object representation, selective attention, conscious recollection, visual perception and associative learning (Basar-Eroglu et al., 1996a,b, 2001b; Tallon-Baudry et al., 1996, 1999; Schurmann et al., 1997; Karakas et al., 2001; Fell et al., 2003). ERO's may therefore be utilized to study specific cognitive effects and also cognitive deficits within a variety of clinical groups. For example, ERO's have been used to study dysfunctions in patients with schizophrenia and ADHD (Yordanova et al., 2001; Gonzalez-Hernandez et al., 2003; Gallinat et al., 2004). In addition it has become a reasonable prospect to identify genes which may control and influence EEG oscillations. Genetic studies can potentially link specific brain neurotransmitter systems with ERO phenotypes which in turn act as correlates of human information processing and cognitive function (Porjesz et al., 2004). Such neurogenetic findings can be expected to help unravel the complex interplay of the neurochemical and neuroanatomical subsystems which are relevant to the generation of brain oscillations evoked under differing cognitive conditions.

It has been demonstrated here that alcoholic subjects show deficits in ERO powers which contribute to the P300 wave. Similar deficits have been observed in a high-risk adolescent population made up from offspring of alcoholic dependent subjects when compared to an age matched low-risk population (Rangaswamy et al., 2005). In addition, θ and δ band ERO's elicited using the Go-Nogo paradigm were observed to be significantly reduced in the frontal, central and parietal regions for the Nogo condition in a group of adult high-risk offspring of alcoholics (Kamarajan et al., 2006). These findings indicate that in a similar way to the P300 amplitude (Begleiter et al., 1984) the condition of reduced theta and δ ERO power may precede the development of alcoholism and therefore represent a trait marker for alcoholism.

The methodology and the findings presented in this paper could be significantly improved upon in many ways. For instance, calculation of the 'current source density' via the surface Laplacian prior to the S-transform TFR decomposition would remove the dependence of the reference electrode. This would allow an easier interpretation of the spatial location of the band-limited power distributions and the location of observed group effects. Also, the location of the time and frequency windows of interest is static and has been defined subjectively by visual inspection of grand-mean TFR plots. Since subjects, trials and electrodes will show differing ERP patterns, a significant improvement could be expected if these windows were defined deterministically at a single trial and single electrode level, per individual. This might be achieved using recently developed time-frequency PCA methods (Bernat et al., 2005). Also, we note that our comparative study uses only the three midline electrodes. These midline electrodes are likely to be suboptimal for examination of the higher frequency components. We can therefore expect improved understanding of ERP group differences through the inclusion of all available electrodes.

5. Conclusion

The results presented here support the view that the P300 'wave' is composed primarily of frontal θ band and posterior δ band oscillatory activity. This observation is in accord with previously published results showing that θ and δ band event-related oscillations underlie the ERP waveform at N200 and P300 latencies and with the notion that these oscillations comprise a parallel processing system of information processing in the brain (Karakas et al., 2000). It is also shown that the evoked δ band oscillatory response, which has a predominantly posterior locus, has close correspondence to the traditional P300 ERP amplitude measure. However, the frontal θ band component of the P300 wave does not have an equivalent ERP amplitude measure and therefore represents novel variable which, in addition to being an important correlate of frontal lobe function (and dysfunction), may provide new clinically relevant information. In this vein we have demonstrated that both the δ and θ band ERO power is reduced in alcoholic subjects when compared to a group of control subjects. These results indicate that for the studied population the total power theta ERO contributes additional discriminatory information to the evoked δ ERO measure. This finding emphasizes the importance of reexamining ERP components in terms of their underlying ensemble of oscillations since new indices of cognitive processing may be illuminated.

Acknowledgements

References

Almasy L, Porjesz B, Blangero J, Chorlian DB, O'Connor SJ, Kuperman S, et al. Heritability of event-related brain potentials in families with a history of alcoholism. Am J Med Genet 1999;88:383–90.

American Electroencephalographic Society. Guidelines for standard electrode position nomenclature. J Clin Neurophysiol 1991;3:38–42.

Basar-Eroglu C, Basar E. A compound P300-40 Hz response of the cat hippocampus. Int J Psychophysiol 1991;60:227–37.

Basar-Eroglu C, Basar E, Demiralp T, Schurmann M. P300-response: possible psychophysiological correlates in delta and theta frequency channels. A review. Int J Psychophysiol 1992;13:161–79.

Basar-Eroglu C, Struber D, Schurmann M, Stadler M, Basar E. Gamma-band responses in the brain: a short review of psychophysiological correlates and functional significance. Int J Psychophysiol 1996a;24:101–12.

Basar-Eroglu C, Struber D, Kruse P, Basar E, Stadler M. Frontal gamma-band enhancement during multistable visual perception. Int J Psychophysiol 1996b;24:113–25.

Basar E, Schurmann M, Sakowitz O. The selectively distributed theta system: functions. Int J Psychophysiol 2001a;39:197–212.

Basar E, Basar-Eroglu C, Karakas S, Schurmann M. Are cognitive processes manifested in event-related gamma, alpha, theta and delta oscillations in the EEG? Neurosci Lett 1999;259:165–8.

Basar E, Basar-Eroglu C, Karakas S, Schurmann M. Brain oscillations in perception and memory. Int J Psychophysiol 2000;35:95–124.

Basar E, Schurmann M, Basar-Eroglu C, Demiralp T. Selectively distributed gamma band system of the brain. Int J Psychophysiol 2001b;39:129–35.

Basar E, Basar-Eroglu C, Karakas S, Schurmann M. Gamma, alpha, delta, and theta oscillations govern cognitive processes. Int J Psychophysiol 2001c;39:241–8.

Basar E, Schurmann M, Demiralp T, Basar-Eroglu C, Ademoglu A. Alpha oscillations in brain functioning: an integrative theory. Int J Psychophysiol 1997;26:5–29.

Begleiter H, Porjesz B, Bihari B, Kissin B. Event-related potentials in boys at risk for alcoholism. Science 1984;225:1493–6.

Berman MS, Whipple SC, Fitch RJ, Noble EP. P3 in young boys as a predictor of adolescent substance abuse. Alcohol 1993;10:69–76.

Bernat EM, Williams WJ, Gehring WJ. Decomposing ERP time-frequency energy using PCA. Clin Neurophysiol 2005;116:1314–34.

Birbaumer N, Elbert T, Canavan A, Rockstroh B. Slow potentials of the cerebral cortex and behavior. Physiol Rev 1990;70:1–41.

Cohen HL, Wang W, Porjesz B, Bauer BO, Kuperman S, O'Connor SJ, et al. Visual P300: An interlaboratory consistency study. Alcohol 1994;11:583–7.

Demiralp T, Ademoglu A, Schurmann M, Basar-Eroglu C, Basar E. Detection of P300 waves in single trials by the wavelet transform (WT). Brain Lang 1999;66:108–28.

Donchin E, Coles MGH. Is the P300 component a manifestation of context updating? Behav Brain Sci 1988;11:357–74.

Doppelmayr M, Klimesch W, Schwaiger J, Auinger P, Winkler T. Theta synchronization in the human EEG and episodic retrieval. Neurosci Lett 1998;257:41–4.

Doppelmayr M, Klimesch W, Schwaiger J, Stadler W, Rohm D. The time locked theta response reflects interindividual differences in human memory performance. Neurosci Lett 2000;278:141–4.

Elbert T, Rockstroh B. Threshold regulation – a key to the understanding of the combined dynamics of EEG and event related potentials. J Psychophysiol 1987;4:314–31.

Fell J, Hinrichs H, Roschke J. Time course of human 40 Hz EEG activity accompanying P3 responses in an auditory oddball paradigm. Neurosci Lett 1997;235:121–4.

Fell J, Fernandez G, Klaver P, Elger CE, Fries P. Is synchronized neuronal gamma activity relevant for selective attention? Brain Res Brain Res Rev 2003;42:265–72.

Fell J, Dietl T, Grunwald T, Kurthen M, Klaver P, Trautner P, et al. Neural bases of cognitive ERPs: more than phase reset. J Cogn Neurosci 2004;16:1595–604.

Folstein MF, Folstein SE, McHugh PR. "Mini-Mental State." A practical method for grading the cognitive state of patients for the clinician. J Psychiat Res 1975;12:189–98.

Freeman WJ. Origin, structure, and role of background EEG activity. Part 1. Analytic amplitude. Clin Neurophysiol 2004a;115:2077–88.

Freeman WJ. Origin, structure, and role of background EEG activity. Part 2. Analytic phase. Clin Neurophysiol 2004b;115:2089–107.

Gabor D. Theory of communications. J Inst Elec Eng 1946;93:429–57.

Gallinat J, Winterer G, Herrmann CS, Senkowski D. Reduced oscillatory gamma-band responses in unmedicated schizophrenic patients indicate impaired frontal network processing. Clin Neurophysiol 2004;115:1863–74.

Gevins A, Smith ME, Leong H, McEvoy L, Whitfield S, Du R, et al. Monitoring working memory load during computer-based tasks with EEG pattern recognition methods. Hum Factors 1998;40:79–91.

Gonzalez-Hernandez JA, Cedeno I, Pita-Alcorta C, Galan L, Aubert E, Figueredo-Rodriguez P. Induced oscillations and the distributed cortical sources during the Wisconsin card sorting test performance in schizophrenic patients: new clues to neural connectivity. Int J Psychophysiol 2003;48:11–24.

Gruber WR, Klimesch W, Sauseng P, Doppelmayr M. Alpha phase synchronization predicts P1 and N1 latency and amplitude size. Cereb Cortex 2005;15:371–7.

Hill SY, Steinhauer SR. Assessment of prepubertal and post pubertal boys and girls at risk for developing alcoholism with P300 from a visual discrimination task. J Stud Alcohol 1993;54:350–8.

Jasper HH. The 10–20 electrode system of the International Federation. Electroencephalogr Clin Neurophysiol 1958;10:371–5.

Kamarajan C, Porjesz B, Jones K, Chorlian D, Padmanabhapillai A, Rangaswamy M, et al. Event related oscillations in offspring of alcoholics: neuro-cognitive disinhibition as a risk for alcoholism. Biol Psychiatry 2006;59:625–34.

Kamarajan C, Porjesz B, Jones KA, Choi K, Chorlian DB, Padmanabhapillai A, et al. The role of brain oscillations as functional correlates of cognitive systems: a study of frontal inhibitory control in alcoholism. Int J Psychophysiol 2004;51:155–80.

Karakas S, Erzengin OU, Basar E. A new strategy involving multiple cognitive paradigms demonstrates that ERP components are determined by superposition of oscillatory responses. Clin Neurophysiol 2000;111:1719–32.

Karakas S, Basar-Eroglu C, Ozesmi C, Kafadar H, Erzengin OU. Gamma response of the brain: a multifunctional oscillation that represents bottom-up with top-down processing. Int J Psychophysiol 2001;39:137–50.

Katsanis J, Iacono WG, McGue MK, Carlson SR. P300 event-related potential heritability in monozygotic and dizygotic twins. Psychophysiology 1997;34:47–58.

Kirschfeld K. The physical basis of alpha waves in the electroencephalogram and the origin of the "Berger effect. Biol Cybern 2005;92:177–85.

Klimesch W. EEG alpha and theta oscillations reflect cognitive and memory performance: a review and analysis. Brain Res Brain Res Rev 1999;29:169–95.

Klimesch W, Schimke H, Schwaiger J. Episodic and semantic memory: an analysis in the RRG theta and alpha band. Electroencephalogr Clin Neurophysiol 1994;91:428–41.

Klimesch W, Doppelmayr M, Pachinger T, Ripper B. Brain oscillations and human memory performance: EEG correlates in the upper alpha and theta band. Neurosci Lett 1997a;238:9–12.

Klimesch W, Doppelmayr M, Schimke H, Ripper B. Theta synchronization and alpha desynchronization in a memory task. Psychophysiology 1997b;34:169–76.

Klimesch W, Doppelmayr M, Russegger H, Pachinger T, Schwaiger J. Induced alpha band power changes in the human EEG and attention. Neurosci Lett 1998;244:73–6.

Klimesch W, Schack B, Schabus M, Doppelmayr M, Gruber W, Sauseng P. Phase-locked alpha and theta oscillations generate the P1–N1 complex and are related to memory performance. Brain Res Cogn Brain Res 2004;19:302–16.

Klimesch W, Doppelmayr M, Yonelinas A, Kroll N, Lazzara M, Rohm D, et al. Theta synchronization during episodic retrieval: neural correlates of conscious awareness. Cognit Brain Res 2001;12:33–8.

Kolev V, Demiralp T, Yordanova J, Ademoglu A, Isoglu-Alkac U. Time-frequency analysis reveals multiple functional components during oddball P300. Neuroreport 1997;8:2061–5.

Kolev V, Yordanova J, Schurmann M, Basar E. Increased frontal phase-locking of event-related alpha oscillations during task processing. Int J Psychophysiol 2001;39:159–65.

Lachaux JP, Chavez M, Lutz A. A simple measure of correlation across time, frequency and space between continuous brain signals. J Neurosci Methods 2003;123:175–88.

Makeig S, Westerfield M, Jung TP, Enghoff S, Townsend J, Courchesne E, et al. Dynamic brain sources of visual evoked responses. Science 2002;295:690–4.

Makinen V, Tiitinen H, May P. Auditory event-related responses are generated independently of ongoing brain activity. Neuroimage 2005;24:961–8.

Mitra PP, Pesaran B. Analysis of dynamic brain imaging data. Biophys J 1999;76:691–708.

Nunez P. Electric fields of the brain – the neurophysics of EEG. New York: Oxford University Press; 1981.

O'Connor SJ, Morzorati S, Christian JC, Li TK. Heritable features of the auditory oddball event-related potential: Peaks, latencies, morphology and topography. Electroencephalogr Clin Neurophysiol 1994;92:115–25.

Penny WD, Kiebel SJ, Kilner JM, Rugg MD. Event-related brain dynamics. Trends Neurosci 2002;25:387–9.

Pfurtscheller G, Lopes da Silva FH. Event-related EEG/MEG synchronization and desynchronization: basic principles. Clin Neurophysiol 1999;110:1842–57.

Pinnegar CR, Mansinha L. A method of time-time analysis: the TT-transform. Digital Signal Process 2003;13:588–603.

Polich J, Herbst KL. P300 as a clinical assay: rationale, evaluation, and findings. Int J Psychophysiol 2000;38:3–19.

Polich J, Pollock VE, Bloom FE. Meta-analysis of P300 amplitude from males at risk for alcoholism. Psychol Bull 1994;115:55–73.

Porjesz B, Begleiter H. Event-related potentials in individuals at risk for alcoholism. Alcohol 1990;7:465–9.

Porjesz B, Jones K, Begleiter H. The genetics of oscillations in the human brain. In: Hallett M, Phillips LH, Phillips LH, Schomer DL, Massey JM, editors. Advances in clinical neurophysiology. Amsterdam: Elsevier; 2004. p. 437–45.

Porjesz B, Begleiter H, Reich T, Van Eerdewegh P, Edenberg HJ, Foroud T, et al. Amplitude of visual P3 event-related potential as a phenotypic marker for a predisposition to alcoholism. Alcohol: Clin Exp Res 1998;22:1317–23.

Porjesz B, Begleiter H. Human brain electrophysiology and alcoholism. In: Tarter R, Thiel DV, editors. Alcohol and the brain. New York: Plenum; 1985. p. 139–82.

Porjesz B, Begleiter H. Effects of alcohol on electrophysiological activity of the brain. In: Begleiter H, Kissin B, editors. Alcohol and alcoholism, the pharmacology of alcohol and alcohol dependence, vol. 2. New York: Oxford University Press; 1996. p. 207–47.

Ramachandran G, Porjesz B, Begleiter H, Litke A. A simple auditory oddball task in young adult males at high risk for alcoholism. Alcohol: Clin Exp Res 1996;20:9–15.

Rangaswamy M, Jones KA, Porjesz B, Chorlian DB, Padmanabhapillai A, Kamarajan C, et al. Delta and theta oscillations as risk markers in adolescent offspring of alcoholics – event related oscillations in visual oddball, 2005. in preparation.

Rohm D, Klimesch W, Haider H, Doppelmayr M. The role of theta and alpha oscillations for language comprehension in the human electroencephalogram. Neurosci Lett 2001;310:137–40.

Sakowitz OW, Schurmann M, Basar E. Oscillatory frontal theta responses are increased upon bisensory stimulation. Clin Neurophysiol 2000;111:884–93.

Sauseng P, Klimesch W, Gruber W, Doppelmayr M, Stadler W, Schabus M. The interplay between theta and alpha oscillations in the human electroencaphalogram reflects the transfer of information between motor systems. Neurosci Lett 2002;324:121–4.

Schurmann M, Basar E. Alpha oscillations shed new light on relation between EEG and single neurons. Neurosci Res 1999;33:79–90.

Schurmann M, Basar-Eroglu C, Basar E. Gamma responses in the EEG: elementary signals with multiple functional correlates. Neuroreport 1997;8:531–4.

Schurmann M, Basar-Eroglu C, Kolev V, Basar E. Delta responses and cognitive processing: single trial evaluations of human visual P300. Int J Psychophysiol 2001;39:229–39.

Shah AS, Bressler SL, Knuth KH, Ding M, Mehta AD, Ulbert I, et al. Neural dynamics and the fundamental mechanisms of event-related brain potentials. Cereb Cortex 2004;14:476–83.

Stampfer HG, Basar E. Does frequency analysis lead to better understanding of human event-related potentials? Int J Neurosci 1985;26:181–96.

Steinhauer SR, Hill SY. Auditory event-related potentials in children at high risk for alcoholism. J Stud Alcohol 1993;54:408–21.

Stockwell RG, Mansinha L, Lowe RP. Localization of the complex spectrum: the S-transform. IEEE Trans Sig Proc 1996;44:998–1001.

Tallon-Baudry C, Bertrand O. Oscillatory gamma activity in humans and its role in object representation. Trends Cogn Sci 1999;3:151–62.

Tallon-Baudry C, Bertrand O, Delpuech D, Pernier J. Stimulus specificity of phase-locked and non-phase-locked 40 Hz visual responses in human. J Neurosci 1996;16:4240–9.

Van Beijsterveldt CEM, Boomsma DI. Genetics of the human electroencephalogram (EEG) and event-related brain potentials (ERPs): a review. Hum Genet 1994;94:319–30.

Van Beijsterveldt T. The genetics of electrophysiological indices of brain activity: an EEG study in adolescent twins. Amsterdam: Universiteit Van Amsterdam; 1996.

van der Stelt O. Visual P3 as a potential vulnerability marker of alcoholism: evidence from the Amsterdam Study of Children of Alcoholics. Alcohol Alcohol 1999;34:267–82.

Varela F, Lachaux JP, Rodriguez E, Martinerie J. The brainweb: phase synchronization and large-scale integration. Nat Rev Neurosci 2001;2:229–39.

Verlerger RG. Event-related potentials and cognition: a critique of the context updating hypothesis and an alternative interpretation of P3. Behav Brain Sci 1988;11:343–56.

von Stein A, Sarnthein J. Different frequencies for different scales of cortical intergration: from local gamma to long range alpha/theta synchronization. Intl J Psychophysiol 2000;38:301–13.

Yeung N, Bogacz R, Holroyd CB, Cohen JD. Detection of synchronized oscillations in the electroencephalogram: an evaluation of methods. Psychophysiology 2004;41:822–32.

Yordanova J, Kolev V. Brain theta response predicts P300 latency in children. Neuroreport 1996;8:277–80.

Yordanova J, Rosso OA, Kolev V. A transient dominance of theta event-related brain potential component characterizes stimulus processing in an auditory oddball task. Clin Neurophysiol 2003;114:529–40.

Yordanova J, Devrim M, Kolev V, Ademoglu A, Demiralp T. Multiple time-frequency components account for the complex functional reactivity of P300. Neuroreport 2000;11:1097–103.

Yordanova J, Banaschewski T, Kolev V, Woerner W, Rothenberger A. Abnormal early stages of task stimulus processing in children with attention-deficit hyperactivity disorder-evidence from event-related gamma oscillations. Clin Neurophysiol 2001;112:1096–108.